BULETINUL INSTITUTULUI POLITEHNIC DIN IAŞI
Publicat de
Universitatea Tehnică „Gheorghe Asachi” din Iaşi
Volumul 65 (69), Numărul 3, 2019
Secţia
ELECTROTEHNICĂ. ENERGETICĂ. ELECTRONICĂ

PERFORMANCE ANALYSIS OF CONSTANT SAMPLING FREQUENCY BASED CURRENT-CONTROLLED INVERTER FED INDUCTION MOTOR DRIVE

BY

CSABA SZABO, ENIKO SZOKE, NORBERT CSABA SZEKELY and VLAD ZACHARIAS*

Technical University of Cluj-Napoca
Faculty of Electrical Engineering

Received: December 20, 2019
Accepted for publication: March 20, 2020

Abstract. The paper deals with a current feedback-based control working at constant sampling frequency for a rotor field orientation-based vector-controlled induction motor drive. The switching signal generated by the current error detector signal is sampled and executed at a constant rate that will ensure the switching frequency limitation reducing the commutation losses in the inverter. Optimal commutation is also possible by shifting the three-phase switching signals in order to avoid simultaneous commutation on the inverter legs. The procedure is characterized by reduced computation and execution time and is suitable for digital implementation. Simulations were performed for different values of the sampling frequency and motor speed, analysing the system behaviour, the current THD and the evolution of the average switching frequency.

Keywords: current-controlled PWM procedure; constant sampling frequency; shifted sampling; vector control; induction motor drive.

1. Introduction

Three-phase Voltage-Source Converters (VSC) are used in a wide range of applications as they can ensure an optimal control of the energy flow

*Corresponding author: *e-mail*: csaba.szabo@emd.utcluj.ro

between the utility AC-line and the connected electrical loads. On the line side may be used as AC-to-DC power supply acting as Voltage-Source-Rectifiers (VSR), usually working with sinusoidal input current with unity power factor control. Current controlled VSC can also be used as active power filter (APF) or active current filter (ACF), also as line-side converter (Suru *et al.*, 2018; Diab *et al*., 2018; Durna, 2016).

In controlled AC electrical drive applications, the three-phase pulse width-modulated (PWM) inverter acts as the actuator for the drive machine. It provides at the output variable frequency and amplitude voltage in order to meet the speed requirement in a wide range ensuring at the same time the magnetization of the machine and also the motor torque. An accurate control of the machine current is of a great importance as it has a direct influence on both the motor torque and flux (Bose, 2006). Optimal control of the AC machines may be achieved by means of based on field-orientation based vector control strategies.

In field-oriented control (FOC) based AC motor drives the control system complexity depends both on the converter control procedure, and the type of the FO that is applied. In industrial applications mostly rotor field orientation (RFO) is used along with open-loop voltage-controlled PWM procedures, like sinusoidal PWM (SPWM) or Space Vector Modulation (SVM) (Bose, 2006). Main advantages of these PWM procedures are the constant switching frequency operation and, the optimal switching process, meaning that in transition between two consecutive switching states only one of the three inverter legs is commutated, which ensures sequential movement of the controlled voltage space vector in a logical order. On the other hand, the corresponding vector control structure has an increased complexity as it requires the computation of the reference voltage for the inverter control. This must be performed in RFO-ed reference frame and it is highly motor parameter dependent. Also, the current control is realized by means of linear controllers that introduce tracking errors and affects the dynamic performances. High system complexity increases both computation and execution times which is an important issue in digital control implementation.

The control system complexity may be significantly reduced when the VSI that feeds the induction motor is controlled by means of a current feedback based PWM technique. The inverter control variable, namely the stator current i_s provided by the flux and speed controllers as two phase RFO-ed components requires only specific transformation coordinate and phase transformations to generate the three-phase sinusoidal reference currents. The absence of the multivariable and parameter dependent voltage computation block and of the two linear current controllers (needed for the voltage-controlled structure) significantly reduces the need on computational resources, improves the dynamic behaviour and reduces to the minimum the parameter dependence of the control system (Kelemen & Imecs, 1991). Due to the above mentioned advantages there is a constant interest regarding the application of current

feedback control in induction motor drives applications (Bose, 1990; Pop *et al.*, 2012; Dey *et al.*, 2013; Ramchand *et al*., 2010; Singh *et al.*, 2018; Peter *et al*., 2018; Talib *et al.,* 2018).

Current-feedback PWM procedures current ensure an accurate control of the current waveform among with peak current and overload protection and superior dynamic performances (Kazmierkowski & Malesani, 1998; Mohseni & Islam, 2010). The classical current-feedback control based on hysteresis regulators are characterized by simplicity, robustness, lack of tracking errors, fast response and independence of load parameter changes. The generated reference current is tracked by the motor current within a hysteresis band. The overall switching frequency and the peak to peak current ripples are influenced by the chosen hysteresis bandwidth.

However, there are several well-known drawbacks of the hysteresis control procedure (Kazmierkowski & Malesani, 1998; Ogudo *et al*., 2019; Bose, 2006).

The control works with variable switching frequency over the fundamental cycle that may generate unwanted harmonics, making it difficult to implement a proper filter and the inverter protections. By narrowing the hysteresis bandwidth, the current ripples are decreased, but undesirable high frequency trigger signals may be generated, leading to high switching frequency that means also increased losses. A large hysteresis bandwidth lowers the switching frequency, but it will increase the current ripples that will be propagated to the motor torque, generating additional noises and mechanical vibrations. It is important to keep a balanced between the peak to peak current ripples and the switching frequency to achieve an optimum performance, considering the characteristics of the controlled process (Bose, 2006; Singh *et al*, 2018).

Researches in the past years are focusing on the optimization of the commutation process in three phase converters (both line and motor side ones) controlled by current-feedback PWM procedures. Many solutions that aim to achieve constant or nearly constant switching frequency are based on variable hysteresis band based on offline or online computation (Bose, 1990; Thepsatorn *et al*., 2006). A generalized model for n-level VSI of a hysteresis controller with an online computed variable current error boundary capable of constant switching frequency is introduced by (Dey *et al*., 2013) for induction motor drive applications. Combination between the online computed variable hysteresis band with the variable sampling period to achieve fixed switching frequency is presented by (Kumar & Gupta, 2016).

Space vector-based solutions also ensure optimal switching process by forcing the current error vector between boundaries of specific shape (Peter *et al*., 2018, Dey *et al*., 2013). Current space-vector procedures are also known as it can achieve optimal commutation by a switching state combination for the three-phase inverter in order to ensure adjacent voltage vector selection.

For large power applications, where high switching frequencies lead to high commutation losses, hysteresis control may be improved also by frequency

limiting procedures applied in order to ensure a minimum switching frequency to ensure stable operation (Ionescu *et al*., 2013; Kazmierkowski, 1998).

This paper deals with two current-feedback procedures for three-phase VSI working at constant sampling rate applied in a vector control structure of a cage induction motor drive. The procedure derives from the classical hysteresis control and is based on the phase current error detection to generate the inverter switching logic. The conventional approach uses the same clock signal for all the three phases to sample the error signals. The second solution uses three different sampling signals for the three inverter legs shifted by one third of the sampling period. By this procedure, the output voltage vector trajectory is similar to the one obtained with voltage SVM, where only adjacent voltage vector selection is allowed that leads to an optimal switching process. Simulations were performed for the motor running at various speed and torque conditions and different sampling frequencies. The behaviour of the control system is analysed both in steady state and dynamic operation as well as the evolution of the computed average switching frequency and the current THD.

2. Current Feedback Control of the VSI at Constant Sampling Frequency

In a classical three-phase three phase inverter topology. Each leg has two branches and each branch has an IGBT and an antiparallel mounted diode. The upper and lower legs are conducting alternatively based on a switching logic. The voltage space-phasor has intermittent motion so that for each one sixth of the fundamental period it corresponds to a fixed position, resulting in a hexagonal-trajectory. For each position it corresponds to a specific, nonzero voltage vector ($\underline{u}_1$ to $\underline{u}_6$). There are also two zero voltage vectors ($\underline{u}_7$ and $\underline{u}_8$) corresponding to the situation when all the upper leg or all the lower leg switching devices are conducting simultaneously. For an optimal commutation the transition between two consecutive states the voltage vector may jump only to an adjacent position or to a corresponding zero voltage state. In this case for the transition only a single inverter leg will be commutated. The classical current-feedback PWM using hysteresis controllers lead to variable switching frequency that may lead in certain operating condition to unwanted, high switching frequency. A simple, cost and computational resource–effective method is based on current error sign detection and ensures switching instants related to an imposed fixed sampling frequency signal. On each phase, the measured currents $i_s(t)$ are compared with the reference sine-wave currents $i_s^{ref}(t)$ generated by the FOC structure, and the error sign will determine the switching logic of the inverter by the following rule (Ionescu *et al.*, 2013; Szabo *et al., 2019*):

$$\begin{cases} sw_{\log} = 0 \text{ for } i(t) \geq i_s^{ref}(t) \\ sw_{\log} = 1 \text{ for } i(t) < i_s^{ref}(t) \end{cases} \tag{1}$$

A suitable method for digital implementation that propose to reduce the switching losses by reducing the switching frequency is based on current error sign detection that will determine the detection and enables switching instants only at fixed sampling intervals.

The switching logic is then sampled by a fixed rate clock signal f_{sp} that will trigger the commutation, applying the corresponding logic signal maintaining its state until the next sampling instant and keeping its state constant. Simple "on-off" controllers are used instead of hysteresis controllers. The maximum possible switching frequency is related to the chosen sampling frequency. However, the method is not capable to ensure constant switching frequency as the switching frequency during a fundamental cycle will still present variations. Depending of the applied sampling procedure there are two cases: the conventional and the shifted sampling approach (Kazmierkowski & Malesani, 1998; Szabo *et al.*, 2019).

2.1. Conventional Sampling Approach

The conventional sampling approach consists in applying the same sampling signal for all the three controller outputs. This method will lead to non-optimal commutation process due to the fact that the switching logics are sampled simultaneously on the three phases. If two or three simultaneous commutation appear the voltage vector may jump to any other position, not only to an adjacent one.

2.2. Shifted Sampling Approach

The conventional sampling procedure can be optimized in order to achieve optimal commutation by using separate sampling signals for each inverter leg being shifted in time with 1/3 of the sampling period, as it can be seen on Fig. 1. Simultaneous commutations are avoided as only one of the three inverter legs can be switched at a time. This will ensure that the transition between two consecutive voltage vector states is made with a minimum number of commutations, allowing switching only between two adjacent states or between a nonzero and a zero voltage state like in case of the classical Space Vector PWM.

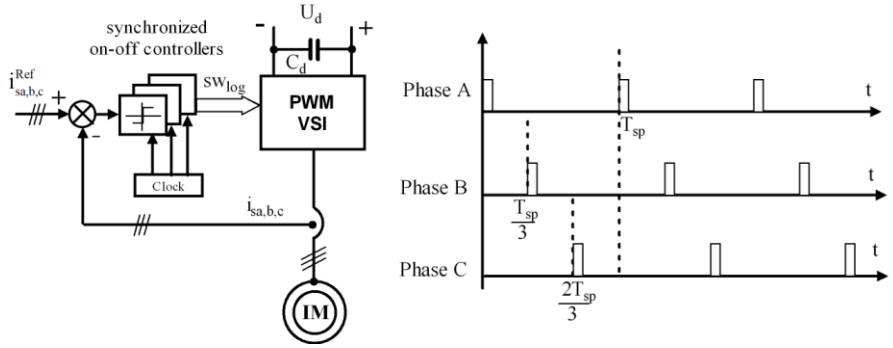

Fig. 1 − The block diagram of the shifted sampling procedure and the distribution of shifted sampling signals (Kazmierkowski, 1998).

In Fig. 2 there is presented the Matlab/Simulink structure of the presented current-feedback procedure working with constant sampling frequency and shifted sampling signals.

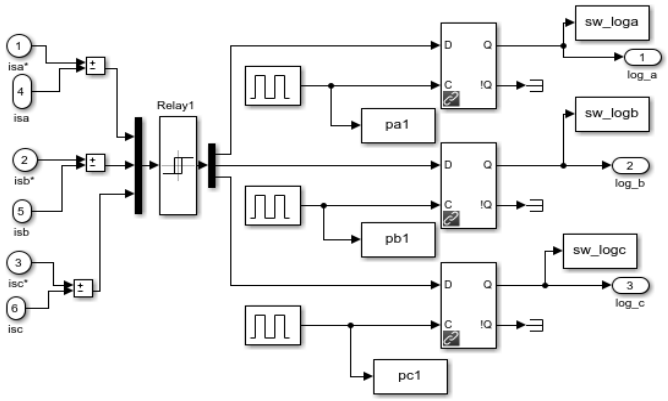

Fig. 2 − Simulink structure of the current-feedback control at constant sampling frequency with shifted sampling (Szabo Cs., *et al*., 2019).

The "Relay" block based on the phase current errors generate at its output the switching logic based on (1) (hysteresis band is set to 0 to reconfigure it to a simple bipositional switch). The obtained signals are then sampled at a fixed rate. On the **"D"** data input of the **D Latch** flip-flop Block there is the initially generated switching logic, i.e. the current error. The chip enable input signal (**C**) controls when the block executes. When **"C"** is greater than zero, the output **"Q"** is the same as the input **"D"**. When the D Latch block is not enabled, the block remains in the previous state (Szabo *et al*., 2019).

3. Rotor-Field-Oriented Control of the Induction Motor

In a vector control structure of an induction machine, based on field-orientation, the independent control of the machine torque and flux (based on the analogy with the DC machine) can be performed on two separate control loops that will indirectly determine the f_s frequency and U_s amplitude of the supply voltage (Bose, B.K., 2006). In Fig. 3 there is presented an RFO-based vector control structure of a squirrel-cage induction machine fed by a three-phase IGBT-VSI controlled by means of carrier-wave current-feedback modulation that ensures constant switching frequency. On the electro-magnetic control loop the Ψ_r rotor-field amplitude is controlled that will influence the amplitude of the supply voltage. On the electromechanical loop the rotor speed is controlled which determine the frequency. For RFO the control is performed in a rotating coordinate frame $(d_{\lambda r} - q_{\lambda r})$ with the direct axis is pointing in the direction of the $\underline{\Psi}_r$ rotor-flux space phasor, where λ_r represents its angular

position related to the stator-fixed (stationary) reference frame. The flux components are:

$$\Psi_{rd\lambda r} = \Psi_r = |\underline{\Psi}_r| \quad \text{and} \quad \Psi_{rq\lambda r} = 0. \tag{2}$$

The flux controller on the reactive loop generates the $i_{sd\lambda r}^{ref}$ reactive stator current component that is equal to the rotor-flux-based magnetizing current i_{mr} (Kelemen & Imecs, 1991; Szabo *et al*., 2019),

$$i_{sd\lambda r} = i_{mr} = \Psi_r / L_m \tag{3}$$

On the active loop the speed controller generates the m_e^{ref} torque reference, while the $i_{sq\lambda r}^{ref}$ active (torque producing) of current component is obtained dividing the reference torque by the reference flux magnitude, as it can be seen in Fig. 3.

The RFO-ed current control variables are transformed into two-phase stator-fixed reference frame by a coordinate transformation (CooT) with matrix operator $[D(\lambda_r)]^{-1}$ then into three-phase components by a reverse phase transformation (PhT with a matrix operator $[A]^{-1}$) obtaining the $i_{sa,b,c}^{ref}$ reference currents for the VSI control. The switching logic of the inverter is then generated based on (1) with either conventional or shifted sampling procedure presented in the previous chapter.

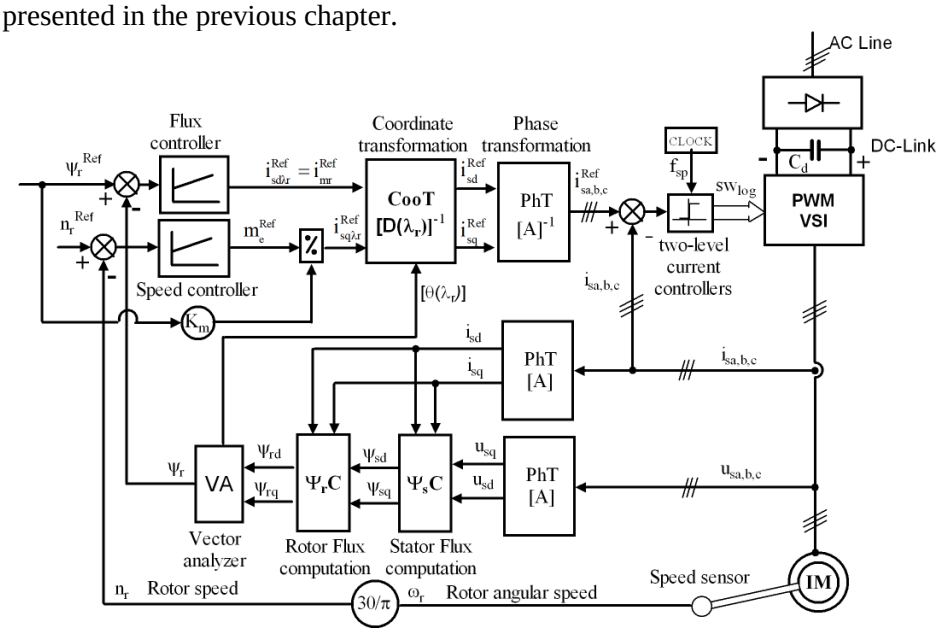

Fig. 3 − Rotor-field-orientation based vector control structure of a squirrel-cage induction motor fed by a VSI controlled with current-feedback modulation at constant sampling frequency.

The rotor flux is identified in two steps based on the following procedure: initially, the stator-flux identification is performed by integration of the back e.m.f. in stator-fixed coordinates, obtaining the two components of the flux space phasor. The rotor flux is then computed by compensation with the leakegy fluxes, resulting the two components of the rotor flux, Ψ_{rd} and Ψ_{rq} in stationary coordinates. That will lead to a direct field orientation, as the analyzer (VA) block computes the $|\Psi_r|$rotor-flux module used as feedback for the flux controller and also identifies the rotor flux space-phasor position λ_r (Kelemen & Imecs M., 1991).

4. Simulation Results

Numerical simulations based on the control structure presented in Fig. 4 were performed in MATLAB-Simulink environment for an existing 2.2 kW, 230 V_{rms}, 50 Hz, 4.7 A_{rms} squirrel-cage induction motor which will be used in future practical implementations. Other rated data: rotor speed n_N = 1415 rpm, electromagnetic torque m_{eN} = 15 Nm, rotor flux Ψ_{rN} = 0.9 Wb. Simulations were performed for both procedures, i.e. the conventional sampling and shifted sampling in same conditions.

The condition imposed by the simulation environment is that any sample time used in the model need to be an integer multiple of the fixed step size used in simulation (*i.e.* $1e^{-6}$ s). In order to meet the condition also for the shifted sampling approach (by considering the delay equals to the one third of the sampling period) the sampling frequency was adjusted accordingly. A series of simulations were performed for three different values of the sampling frequency: 33.3 kHz, 16.7 kHz, and 11.1 kHz. The motor is started by applying a reference speed of 1415 rpm at rated load torque of m_L= 15 Nm, results being shown in Fig. 4 for both sampling procedures.

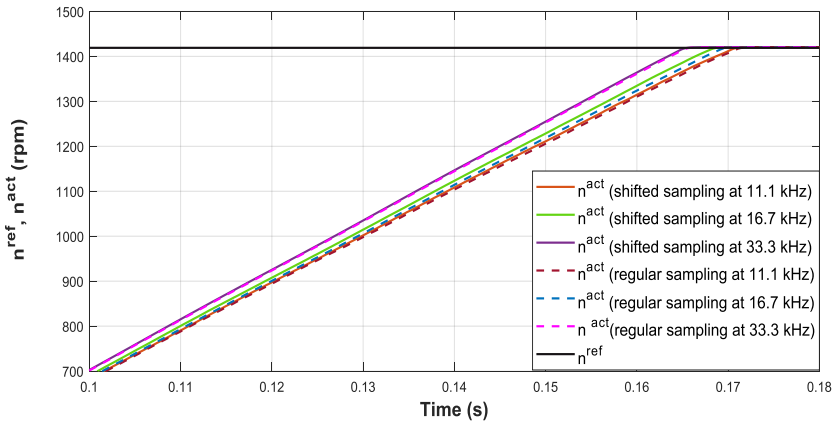

Fig. 4 – Rotor speed evolution at the end of the starting process for regular and shifted sampling at different sampling frequencies (n^{ref} – reference speed, n^{act} – actual speed).

Smaller settling times for both methods are obtained for higher sampling frequencies. For a sampling frequency of 33.3 kHz the speed response is almost identical for the two methods.

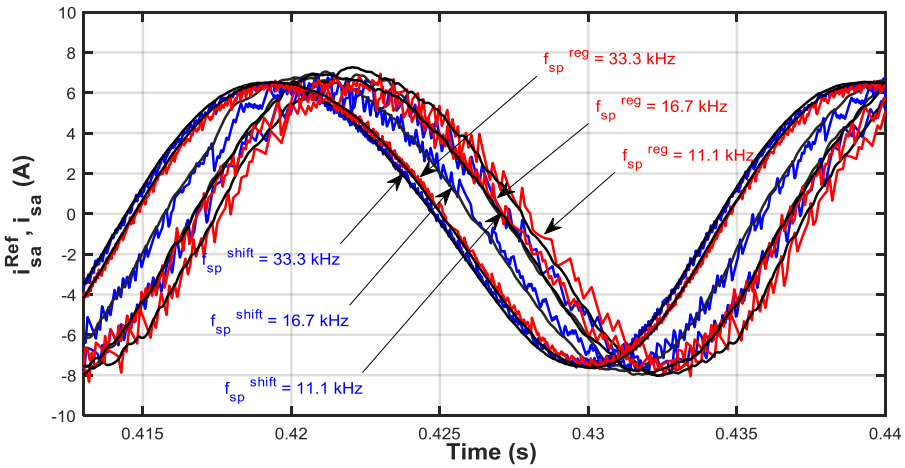

Fig. 5 – Stator current in phase *a* in steady-state operation for different sampling frequencies: (shift – for shifted sampling; reg – for regular sampling).

In Fig. 5 may also be observed that there is a phase shift between the sator currents that are directly related to this difference in the settling times from Fig. 4. Also, as it was expected, the current distortion decreases as the sampling frequency is increasing. As the current is less distorted at higher sampling frequency, the curent amplitude also becames smaller, meaning that the efficiency is increasing. Fig. 6 presents the stator voltage space phasor that shows the random transition between the consecutive switching states for the conventional sampling and the optimal transition with sequential movement between adjacent voltage vector states for the shifted sampling method.

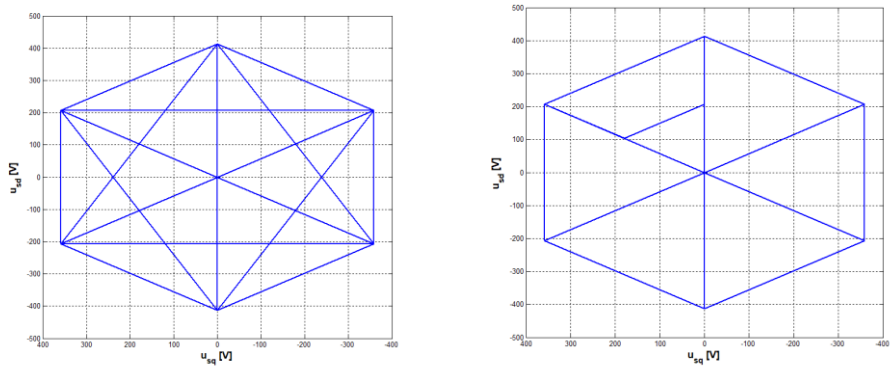

a *b*

Fig. 6 – The stator voltage space-phasor for: *a* – regular sampling; *b* – shifted sampling.

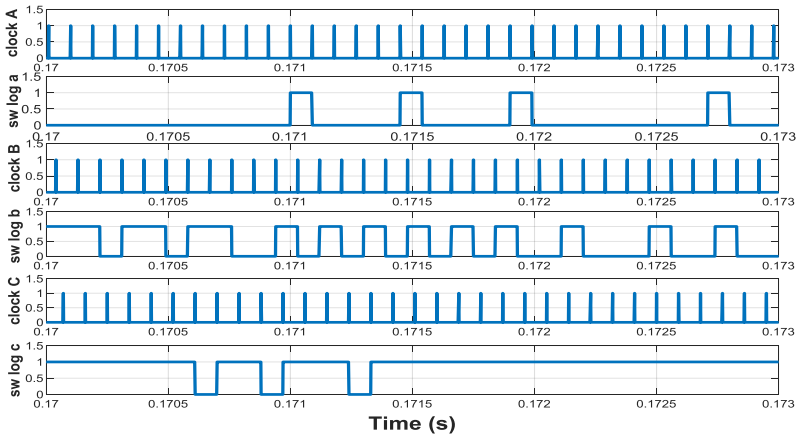

Fig. 7 – The shifted clock signals and the sampled logic signals for 11.1 kHz sampling frequency, running at 1415 rpm, for shifted sampling.

Fig. 7 shows the inverter switching logic signals sampled by the three shifted signals, thus disallowing simultaneous commutations, which leads to optimal commutation.

In Table 1 are presented the results obtained by FFT performed on the motor current in phase *a* for a fundamental cycle, showing the current magnitude and the Total Harmonic Distortion (THD). Both sampling techniques were analyzed for different sampling frequencies, (33.3 kHz, 16.7 kHz and 11.1 kHz) and three different running speeds. The motor was running at 15 Nm load.

Table 1
Current THD

Speed (rpm)	Sampling frequency (kHz)	Fundamental frequency (Hz)	Conventional sampling		Shifted sampling	
			Magnitude (A)	THD (%)	Magnitude (A)	THD (%)
1,415	33	50	6.828	8.50	6.837	8.56
707		26	6.849	4.74	6.85	4.6
280		12	6.851	3.12	6.852	3.07
1,415	16.7	50	6.83	9.31	6.841	9.61
707		26	6.839	6.82	6.844	6.34
280		12	6.846	5.55	6.853	5.52
1,415	11.1	50	6.839	10.78	8.855	10.9
707		26	6.819	9.39	6.83	8.27
280		12	8.837	8.27	6.847	7.05

As it was expected, THD decreases when the sampling frequency is increasing, but the increase of the rotor speed leads to higher THD values. The

distortion factor is always higher at nominal speed, but the gap between the THD values became more pronounced at high sampling frequency, where at high speed and full load the motor current is not able to closely track the reference current due to the high back e.m.f. value which becomes equal or even higher than the supply voltage. In this case the current is switched only once per period.

Table 2
Computed average switching frequency

Speed (rpm)	Sampling frequency (kHz)	Average switching frequency [Hz]			
		Regular sampling		Shifted sampling	
		15 Nm load	2 Nm load	15 Nm load	2 Nm load
1415	33	7600	7640	7730	7740
707		11700	11800	11650	11890
280		14400	14720	14350	14690
1415	16.7	3770	3780	4000	3970
707		5800	5850	5770	5900
280		7140	7300	7130	7270
1415	11.1	2620	2610	3900	3850
707		3800	3840	3780	3790
280		4690	4820	4620	4740

This may be observed also on the current waveforms from Fig. 6.

In Table 2 there are shown the average switching frequencies obtained in same working conditions as the results presented for the THD, but in addition the values are computed not only for a 15 Nm full load, but also for no load running, at 2 Nm. The load variation does not significantly affect the switching frequency. As expected, the switching frequency is always less than a half of the sampling frequency and it is close to that value at low speed range, presenting a significant decrease as the rotor speed approaches the nominal value.

4. Conclusions

The paper presents an analysis of a current-feedback control of a VSI for FOC based variable speed induction motor drive. It offers a simpler control structure than the ones that use voltage PWM for the inverter control and also ensures superior dynamic performances. The current controlled PWM ensures an accurate current control without tracking errors providing also overload protection.

The current feedback procedures for VSI presented in this paper are working at constant sampling rate that brings improvements to the classical hysteresis control working with variable, uncontrolled switching frequency. By limiting the switching frequency, it significantly cuts the switching losses.

Optimal commutation process may be achieved by shifting the sampling signals with one third of the sampling period in order to avoid simultaneous commutations on the inverter lag. By doing this, the voltage space phasor will have a sequential motion, same as in case of open-loop voltage controlled procedures by allowing only adjacent or zero voltage vector selection in the transition process between two consecutive states.

Acknowledgments. The results presented in this paper were obtained in the framework of the GNaC 2018 ARUT grant "Optimization of Current-Feedback PWM Procedures for Three-Phase Power Electronic Converters", research Contract no. 3046/05.02.2019, with the financial support of the Technical University of Cluj-Napoca.

Part of research from this article was presented at the 12th International Conference and Exhibition on Electromechanical and Energy Systems, Sielmen 2019, event co-organized by Faculty of Electrical Engineering, Gheorghe Asachi Technical University of Iaşi.

REFERENCES

Bose B.K., *An Adaptive Hysteresis-Band Current Control Technique of a Voltage-Fed PWM Inverted for Machine Drive System*, IEEE Trans. Ind. Electron., **37**, 402-408 (1990).

Bose B.K., *Power Electronics and AC Drives*, PrenticeHall, New Jersey, N.J, 2006.

Dey A., Azeez N.A., Gopakumar K., Kazmierkowski M.P., *Simple Computation Techniques of Online Boundary to Achieve Constant Switching Frequency in any General n-level VSI fed IM Drive Using Hysteresis Current Controller*, Proc. Of the IEEE International Conference on Industrial Technology, ICIT 2013, 25-28 Feb. 2013, Cape Town, South Africa, Published by IEEE, Print ISBN: 978-1-4673-4567-5, 404-409.

Diab M., El-Habrouk M., Abdelhamid T.H., Deghedie S., *Survey of Active Power Filters Configurations*, 2018 IEEE International Conference on System, Computation, Automation and Networking (ICSCA 2018), 6-7 July 2018, Electronic ISBN: 978-1-5386-4866-7.

Durna E., *Effect of Sampling Frequency and Execution Time on Hysteresis Current Controlled Three-Phase ThreeWire HAPF Converters*, 2016 International Symposium on Power Electronics, Electrical Drives, Automation and Motion (SPEEDAM 2016), Capri, Italy, 22-24 June 2016, 812-824.

Gao M., Ji Y., Wang J., *Improved Ramptime Current Control Strategy*, Proc. Of 5th International Conference on Information Science and Control Engineering, ICISCE 2018, 20-22 July 2018, Zhengzhou, China, Published by IEEE, E1. ISBN: 978-1-5386-5500-9, 786-790.

Ionescu (Pop) A.V., Imecs M., Incze I.I., Szabo Cs., *Performance Analysis of Three Current-Controlled PWM-Procedures Applied in Vector Control of Induction Machine Drives*, Proceedings of the 4th International Conference on Recent Achievements in Mechatronics, Automation, Computer Sciences and Robotics MACRo2013, Tg. Mures, Romania, 2013, ISSN 2247-0948, pp. 143-153.

Kazmierkowski, M.P., Malesani, L., *Current control techniques for three-phase voltage-source PWM converters: a survey*, Industrial Electronics, IEEE Transactions on, **45**, 691-703 (1998).

Kelemen A., Imecs M., *Vector Control of AC Drives.* Volume **1***: Vector Control of induction Machine Drives*, Budapest: Omikk Publisher, ISBN 963-593-140-9, 1991.

Kumar M., Gupta R., *Sampled-Time-Domain Analysis of a Digitally Implemented Current Controlled Inverter*, IEEE Transactions on Industrial Electronics, **64**, *1***,** 217-227 (2016).

Mohseni M., Islam S. M., *A New Vector-Based Hysteresis Current Control Scheme for Three-Phase PWM Voltage-Source Inverters*, IEEE Transactions on Power Electronics, **25**, 2299-2309 (2010).

Ogudo K.A., Makhubele J. W., *Comparative Analysis on Modulation Techniques For a Single Phase Full-Bridge Inverter on Hysteresis Current Control PWM, Sinusoidal PWM and Modified Sinusoidal PWM*, Proc. Of the International Conference on Advances in Big Data, Computing and Data Communication Systems icABCD 2019, 5-6 Aug. 2019**,** Winterton, South Africa, Published by IEEE, El. ISBN: 978-1-5386-9236-3.

Peter J., Shafi M.K.P., Lakshmi R., Ramchand R., *Nearly Constant Switching Space Vector Based Hysteresis Controller for VSI Fed IM Drive*, IEEE Trans. on Ind. Appl., **54**, *4* (2018).

Pop A.V., Imecs M., Incze I.I., Negrea C.A., *Modeling and Simulation of Current-Controlled PWM Strategy with Regular Sampling for Constant Switching Frequency*, Proceedings of the 2012 International Conference and Exposition on Electrical and Power Engineering (EPE 2012), Iaşi, 2012, DOI 10.1109/ICEPE.2012.6463589, pp. 446-450.

Ramchand R., Sivakumar K., Das A., Patel C., Gopakumar K., *Improved switching frequency variation control of hysteresis controlled voltage source inverter-fed IM drives using current error space vector*, IET Power Electronics, **3**, *2*, 219-231 (2010).

Singh M., Sreejeth M., Devanshu A., *Comparative Performance Analysis of IVCIM Drive using different Gain values of PI and Band values of Hysteresis Band Controller*, Proc. Of the International Conference on Power Energy, Environment and Intelligent Control, PEEIC 2018, 13-14 April 2018, Greater Noida, India, Published by IEEE, E1. ISBN: 978-1-5386-2341-1, 132-137.

Suru C.V., Popescu M., Preda C.A., *Constant Frequency Hysteresis Controller Implementation For Active Filtering Systems*, Bul. Inst. Politehnic, Iaşi, **LXIV**(**LXVIII**), *2*, s. Electrot., Energ., Electron., 19-38 (2018).

Szabo Cs.. Szoke E., Szekely N.Cs, Zacharias V., *Current-Feedback Control at Constant Sampling Frequency Applied in Rotor-Field-Oriented Induction Machine Drives*, 2019 International Conference on Electromechanical and Energy Systems SIELMEN 2019, 9-11 Oct. 2019, Published by IEEE, Electronic ISBN: 978-1-7281-4011-7.

Talib M.H.N., Mat Isa S.N., Hamidon H.E., Ibrahim Z., Rasin Z., *Hysteresis Current Control of Induction Motor Drives Using dSPACE DSP Controller*, Proc. Of IEEE International Conference on Power and Energy, PECon 2016, 28-29 Nov. 2016, Melaka, Malaysia, Published by IEEE, E1. ISBN: 978-1-5090-2547-3, 522-527.

Thepsatorn P., Sodaban C., Tipsuwanporn V., Jitnaknan P., *Improvement Signal Output of DM–PWM Inverter for Driving High-Efficient Electrical Load*, Proc. IEEE Power Electron. Motion Control Conf. 2006, pp. 913-918.

Wu F. , Feng F., Luo L. , Duan J, Sun L., *Sampling Period Online Adjusting-Based Hysteresis Current Control Without Band With Constant Switching Frequency*, IEEE Trans. on Ind. El., **2**, *1* (2015).

ANALIZA PERFORMANŢEI UNUI SISTEM DE ACŢIONARE A MOTORULUI DE INDUCŢIE ALIMENTAT DE LA UN INVERTOR CU COMANDĂ ÎN CURENT CU PAS DE EŞANTIONARE CONSTANT

(Rezumat)

Lucrarea analizează procedura de comandă în buclă închisă de curent a unui invertor de tensiune care alimentează o maşină de inducţie controlată vectorial. Logica de comandă generată în urma detecţiei erorii de curent este eşantionată de un semnal de frecvenţă constantă care limitează frecvenţa de comutaţie a invertorului permiţând comutaţii doar la perioade de timp constante. Procedura este simplă, timpii de calcul şi de execuţie fiind reduşi, pretându-se astfel implementării pe dispozitive de calcul digitale. S-au efectuat simulări pentru procedeele vizate analizându-se componenţa în armonici a curentului motorului cât şi evoluţia frecvenţei de comutaţie medie calculată pentru diverse valori ale frecvenţei de eşantionare şi la viteze de funcţionare diferite.